Eur Radiol (2004) 14:184–192
DOI 10.1007/s00330-003-2142-y

I. Van Breuseghem

Ultrastructural MR imaging techniques of the knee articular cartilage: problems for routine clinical application

Received: 22 May 2003
Revised: 31 July 2003
Accepted: 1 October 2003
Published online: 5 November 2003

I. Van Breuseghem (✉)
Department of Radiology,
University Hospitals Leuven,
Herestraat 49, 3000 Leuven, Belgium
e-mail:
Iwan.Vanbreuseghem@uz.kuleuven.ac.be
Tel.: +32-16-343770
Fax: +32-16-342470

Abstract The high incidence of cartilage lesions together with new surgical treatment techniques have necessitated the development of non-invasive cartilage evaluation techniques. Although arthroscopy has been the standard for cartilage evaluation, MR imaging has emerged as the imaging method of choice, allowing morphological evaluation of cartilage and cartilage repair tissue, as well as evaluation of its biochemical content. This article deals with current ultrastructural MR imaging techniques for cartilage evaluation, indicating the advantages as well as the drawbacks for routine clinical application.

Keywords Cartilage · MR imaging · Knee · Osteoarthritis

Introduction

Injuries and degenerative changes in the articular cartilage are a significant cause of morbidity and diminished quality of life, with osteoarthritis ranking second only to cardiovascular disease as a cause of work-related disability [1]. Because of this high incidence of cartilage damage and thanks to new surgical cartilage repair procedures, the evaluation of articular cartilage has gained increasing attention in the scientific community. Although arthroscopy has been the gold standard for diagnosing and monitoring cartilage damage and repair, it is less than optimal for several reasons. It is invasive and expensive. Moreover, it only allows visual inspection of the cartilage surface, enforcing additional evaluation (e.g., physically probing the cartilage) to find hidden defects within the midsubstance of the tissue.

Although several imaging methods exist for cartilage evaluation, MR imaging of cartilage has been shown to be accurate for the detection of chondral abnormalities [2, 3, 4, 5, 6, 7, 8] and in evaluating cartilage-repair procedures [9, 10, 11].

Apart from the evaluation of morphological defects, certain MR imaging contrast mechanisms have shown to reveal detailed information regarding the biochemical content (ultrastructure) of cartilage.

This article deals with the current available ultrastructural MR imaging techniques related to their biochemical target, indicating the advantages as well as the drawbacks for routine clinical application. For a good understanding of these imaging techniques a brief discussion on cartilage anatomy is given.

Structure of articular cartilage

Articular cartilage is a complex tissue—avascular, aneural, and alymphatic—that relies on diffusion of solutes

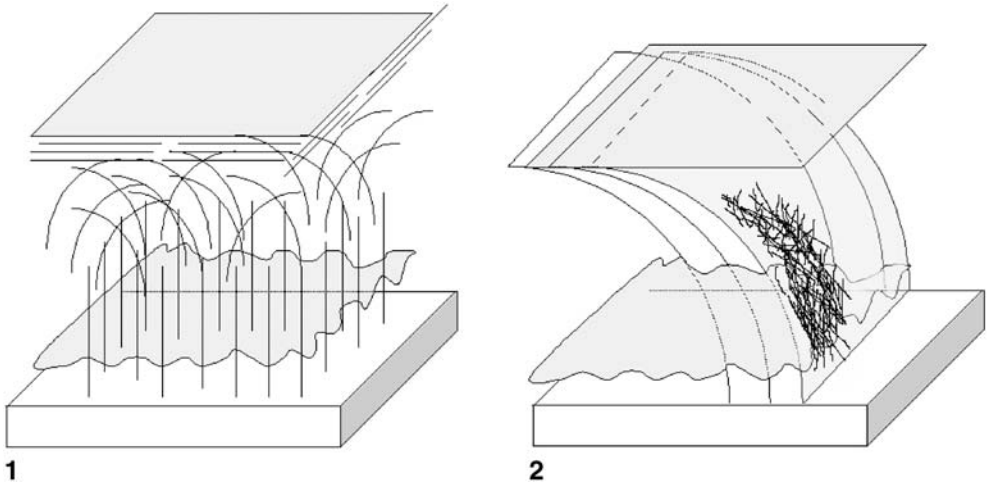

Fig. 1 Articular cartilage organized as a layered structure: cartilage can be divided into four anatomical zones. This is related to the collagen orientation, which is horizontal near the articular surface (*top*), random in the second layer, and vertical in the deeper half of the cartilage near the subchondral bone (*bottom*). The vertical layer consists of a non-calcified (*upper*) part and a calcified (*lower*) part, divided by the *tide mark*

Fig. 2 Leaf-like collagen architecture organization, based on scanning electron microscopy findings. The leaves contain randomly organized collagen fibrils

for its cellular nutrition [12]. These highly specialized cells produce the extracellular matrix, responsible for the properties of articular cartilage. This matrix is composed of three major constituents: water; collagen; and proteoglycan aggregates [12, 13, 14]. Water comprises approximately 75% of the wet cartilage weight, which is either freely moving throughout the matrix or reversibly bound to the macromolecules. Of those macromolecules, collagen comprises a major constituent making up approximately 20% of cartilage volume by weight. Collagen in hyaline cartilage is primarily type II, providing cross reaction between collagen molecules and thus creating a very stable framework that resists tensile forces. The proteoglycan macromolecule, which makes up approximately 5% of cartilage volume by weight, has a "bottlebrush" appearance by electron microscopy. It is composed of a central core protein to which are bound sulfated glycosaminoglycans (GAG). Of functional importance are the negative charges of this molecule and its hydrophilic character: they provide resistance to fluid flow and a considerable compressive strength [12, 13, 14]. According to light microscopy findings, cartilage is divided in different anatomical zones related to the anatomical distribution and orientation of collagen (Fig. 1) [15]. The most superficial zone, also called the tangential zone, contains thin collagen fibers oriented parallel to the joint surface. Deep to this zone is the transitional zone, in which collagen fibers are randomly organized. The deepest zone is called the radial zone, in which the thickest fibers are found, oriented perpendicular to the articular surface. It is divided by the "tide mark" in a superficial noncalcified layer and a deeper calcified layer. Subchondral bone is found deep to the calcified layer.

Scanning electron microscopy performed after freeze-fracture sectioning shows the three-dimensional structure of the collagen network [16, 17] and has put the aforementioned light microscopy model into new perspective. Matrix collagen within cartilage is organized in continuous leaf-like structures that radiate from the subchondral interface in a perpendicular orientation and then curve into the horizontal orientation at the articular surface (Fig. 2). Moreover, within the leafs the orientation of individual collagen fibers appears random in all regions. No qualitative difference can be made in the orientation of collagen fibers in the different layers as determined by the light microscopy model [18]. This scanning electron microscopy cartilage model supports a complex three-dimensional organization of the collagen network which can explain the different layers seen on MR images (see later in the discussion on differences in T2 decay and the magic-angle effect).

The overall functional integrity of cartilage is determined not only by the solid/fluid volume fraction, collagen composition, molecular structure and organization, and GAG composition, but also on their interdependent effects. Although the exact pathophysiological mechanisms for cartilage damage still need to be determined, one can intuitively understand that each matrix component is involved and has determinative effects on the others.

Ultrastructural MR imaging techniques for articular cartilage

The ultrastructural imaging techniques for articular cartilage evaluate its macro-molecular and water content. Different techniques exist for each component and are grouped accordingly for the discussion herein (Table 1).

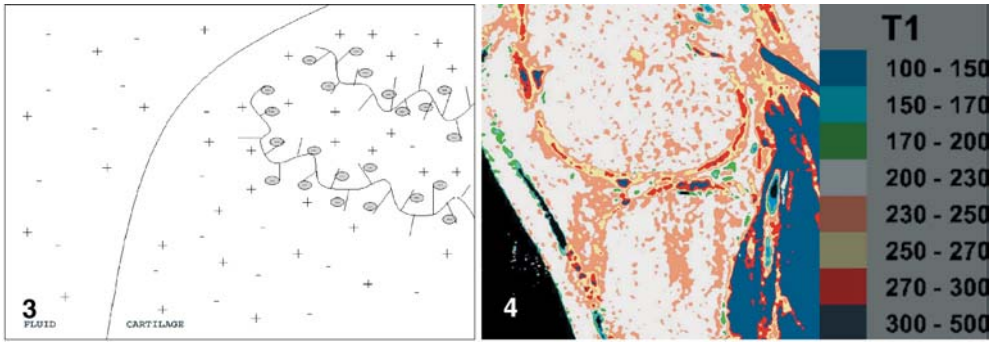

Fig. 3 Distribution of charged ions in cartilage and synovial fluid. The proteoglycan component is represented as a black backbone with charged negative glycosaminoglycans (GAG) side groups. Because of this fixed negative charge, the distribution of gadopentate dimeglumine will be in lower concentration in normal cartilage (*upper*) than in synovial fluid and GAG-depleted cartilage (*lower*)

Fig. 4 In vivo T1-calculated image (dGEMRIC image; multi-inversion recovery sequence: TR 1800 ms/TE74 ms/TI 25–1600 ms) of a knee 2 h after IV administration of contrast after color-encoded image post-processing, with spatial differences in T1 relaxation time reflecting spatial differences in GAG distribution

Table 1 Overview of different techniques for ultrastructural cartilage imaging and their relationship with the major constituents of the cartilage matrix. *dGEMRIC* delayed gadolinium-enhanced magnetic resonance imaging of cartilage

Matrix constituent	Imaging technique
Proteoglycan	dGEMRIC T1ρ mapping ^{23}Na spectroscopic imaging T2 mapping
Collagen	T2 mapping Magnetization transfer mapping Magic-angle imaging
Interstitial water	T2 mapping Proton density (ρ) mapping Diffusion imaging and fractional anisotropy

The first group of techniques are related to the proteoglycan (GAG) content of articular cartilage and comprise delayed gadolinium-enhanced MR imaging of cartilage (dGEMRIC), T1ρ imaging, and sodium MR spectroscopy.

dGEMRIC

Glycosaminoglycans are the main source of tissue fixed charge density (FCD) in cartilage, which are lost in the event of cartilage degeneration. Intra-venous administered gadopentate dimeglumine (Gd-DTPA^{2-}) penetrates the cartilage through both the articular surface and the subchondral bone. The contrast equilibrates in inverse relation to the FCD, which are in turn directly related to the GAG concentration (Fig. 3); therefore, T1, which is determined by the Gd-DTPA^{2-} concentration, becomes a specific measure of tissue GAG concentration [19]. Without Gd-DTPA^{2-}, T1 did not change significantly even with complete loss of GAG. Even so T1 differences noted with Gd-DTPA^{2-} were not seen with a non-ionic Gd-compound (e.g., Gadoteridol) [20]. This makes the tissue T1 after Gd-DTPA^{2-} administration a sensitive and specific indicator of relative FCD.

In practice, cartilage T1 is high in normal cartilage and low in GAG-depleted, osteoarthritic cartilage. The T1 value is determined using a multi-inversion recovery turbo-spin-echo imaging series, followed by curve fitting the T1 images to generate T1 maps. Color or gray-scale post-processing of these T1 maps is widely used to render the images de visu interpretable (Fig. 4). The value of this technique and the possible clinical applications have been repeatedly emphasized in the literature [21, 22, 23, 24].

The observed differences in calculated T1 values between different research groups (ranging from 300 to 580 ms for normal cartilage and 210 to 360 ms for diseased cartilage), however, deserve some attention [20, 22, 23, 26]. An explanation for these differences is not readily available. A possible cause could be the use of different field strengths (which is not the case in above-mentioned studies, all performed at 1.5 T): an increase in T1 values is noted with increasing field strength [27].

A second issue concerns the "relaxivity" of Gd-DTPA^{2-}: relaxivity is defined as the change in relaxation rate of contrast agent. Studies revealed the relaxation rate of Gd-DTPA^{2-} to be temperature dependent as well as field-strength dependent. When not corrected, this change in relaxivity introduces errors in the T1 relaxation rate especially at lower field strengths [28]. Thirdly, the mathematical algorithm used to calculate T1 may account for observed differences. Fourthly, some protocol issues for practical clinical application of this technique have been described [22]: a double dose of Gd-DTPA^{2-} should be injected intravenously, followed by an immediate active-joint exercise period. T1 relaxation measurements should be performed 2–3 h post-injection. Color mapping of T1 calculated images is appropriate to

discern variations in T1 across the tissue. Incoherencies in the applications of these issues introduces T1 differences.

As stated previously, T1 of cartilage in the presence of Gd-DTPA^{2-} is a good indicator of relative FCD. If information on the absolute FCD (and thus GAG concentration) is desirable, an electrochemical model must be used [19]. The knowledge of absolute FCD, however, seems of relative importance in practical clinical applications, as it can be compared with known normal T1 relaxation rates.

T1ρ imaging

T1ρ imaging is a new technique especially in the field of cartilage imaging: T1ρ imaging means spin-lattice relaxation in the rotating frame and is characterized by the time constant that defines the magnetic relaxation of spins under the influence of a radio-frequency field (T1ρ). Changes in T1ρ were observed in chemically proteoglycan-depleted cartilage plugs but not in collagenase-treated tissue [29, 30]. Recently, the application of this technique in a 1.5-T MR imaging system was described [31]. A strong correlation exists between proteoglycan loss and increase in T1ρ relaxation time, not noted with collagen loss, making it a sensitive and specific method. T1ρ imaging can therefore be used to map the proteoglycan distribution in cartilage.

T1ρ imaging seems to provide a convenient method to evaluate the slow-motion components that cause relaxation. These slow-motion processes seem to play a larger role in cartilage T1ρ compared with that of muscle [31]. The exact physical mechanisms responsible for this type of dispersion behavior are not well known, so further research needs to be done to determine and separate these mechanisms.

T1ρ imaging can be obtained by preparing the magnetization with a spin-locking prepulse followed by a standard fast-spin-echo (FSE) sequence [31]. Although the clinical usefulness of this technique is not yet established well in literature, T1ρ imaging could serve as an attractive alternative to the dGEMRIC method in the future. In comparison with the dGEMRIC method, T1ρ imaging does not require intravenous injection of contrast agent, no joint exercise nor a time-delay period of 2 h before imaging.

Na-23 spectroscopic imaging

Sodium MRI is a recently described new technique for cartilage imaging. Its utility is based on the ability of sodium imaging to depict regions of proteoglycan depletion [32]. According to the same principle as described for dGEMRIC imaging, ^{23}Na atoms are associated with the FCD present in GAG. Because of the inherent positive charged ^{23}Na, there is a direct relationship between local ^{23}Na concentration and FCD. Some spatial variation in ^{23}Na concentration seems present within normal cartilage and in cartilage samples.

Sodium imaging has been shown to be sensitive to small changes in proteoglycan concentration [33]. There is a substantial reduction (~50%) in image intensity in enzymatic GAG-degraded regions compared with the nondegraded regions [32]; however, despite these promising results, the application of this technique in routine clinical cartilage imaging seems precluded since it requires special hardware modifications (e.g., preamplifier for sodium frequency, double-tuned coils), not available on routine clinical MR imaging systems.

The second group of techniques are related to the collagen content of cartilage and comprise T2-mapping, magnetization transfer (MT) imaging, and magic-angle imaging.

T2 mapping

T2 mapping of articular cartilage is a widely discussed technique in the literature, demonstrating its value in the evaluation of early (ultrastructural) cartilage damage [34, 35, 36, 37, 38, 39, 40, 41, 42]. There is, however, no consensus on the ultrastructural components determining the T2 value of cartilage: this makes T2 mapping of cartilage a sensitive although non-specific technique. The vast majority of authors agree on the major contribution of collagen orientation (determined by the magic-angle effect) and collagen concentration to the T2 value [34, 35, 38, 39, 40]. Some authors indicate a significant additional contribution from proteoglycan and water content [36, 37, 41]. All authors, however, agree that ultrastructural cartilage damage is associated with an increase in T2 relaxation time, which is important for practical clinical applications.

As already mentioned, the magic-angle effect is a major determinant in the T2 behavior of cartilage, explained by the anisotropic motion of water molecules parallel to the direction of collagen fibers. Spin-spin coupling (T2) is mediated by the inter-spin distance and by the respective magnetic fields of each proton, which are characterized by the term $(3\cos^2\theta\text{-}1)$. θ is the angle between the main magnetic field (B_0) and a vector through adjacent protons [43]. In isotropic tissues, where water is freely moving, this angular dependence averages to zero. With the angular anisotropy of water molecules along the collagen fibers, however, a net angular dependence remains, leading to anisotropic T2. With this anisotropy, spin-spin coupling is minimized (i.e., T2 is maximal) at the angles where $(3\cos^2\theta\text{-}1)=0$. This corresponds to θ=54.7°, 125.3°, 234.7°, or 305.3°, with θ=54.7° called the magic angle (θ_m). Applied to cartilage, with its highly orga-

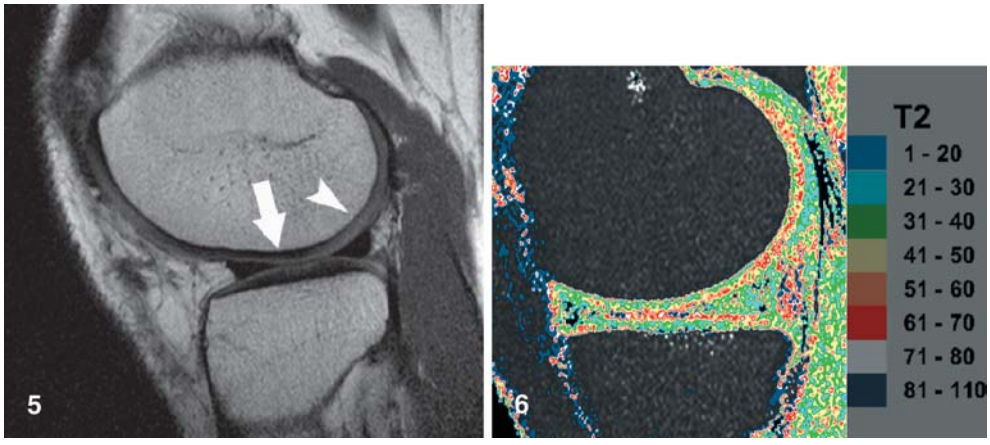

Fig. 5 Proton-density fast-spin-echo-weighted sagittal image (TR 2000 ms/TE35 ms) through the lateral femoral condyle showing the layered cartilage appearance in the weight-bearing cartilage area (*arrow*) which disappears more posteriorly (*arrowhead*) related to the magic-angle effect

Fig. 6 In vivo calculated T2 map of articular cartilage, using a multi-echo spin-echo sequence (TR 1500 ms/TE9–99 ms in 9 ms increments/1.5 T). A color-encoded look-up table is shown on the *right*, from which the T2 dependence of cartilage as a function of tissue depth and orientation with respect to B_0 is seen

Table 2 Resulting T2 values as presented by different authors. The cartilage was arbitrarily divided in a deep and superficial portion, from which mean T2 values were calculated in order to demonstrate spatial differences in T2 relaxation times

Reference	Technique	T2 deep (ms)	T2 superficial (ms)
[48]	In vitro bovine patella	51	77
[52]	In vitro bovine patella	20	55
[35]	In vivo human patella	32	67
[37]	In vivo human patella	30	65
[42]	In vivo human femur/tibia	46	56

nized collagen matrix, T2 is heterogeneous, anisotropic, and dependent on the tissue depth [44]: T2 of cartilage is therefore a local parameter, associated with the local structure of the tissue and orientation dependent. This is nicely demonstrated by Mosher et al. [45, 46, 47].

The laminar appearance of cartilage on MRI is a direct consequence of the T2 anisotropy, with the effect of lamination being most apparent at 0° and almost invisible around θ_m (Fig. 5). Depending on the authors studying the laminar appearance of cartilage, two to four layers could be discerned [48, 49, 50]. In an attempt to explain these differences, artifacts (truncation, chemical shift) and technical issues (i.e., resolution) were suggested. In correlating the laminae seen on MR images with light microscopy findings, Modl et al. [49] found a correspondence in location but not in thickness. The MR images and scanning electron microscopy on the contrary seem well correlated: MR layers correlate well with the curvature of the fractured samples and not at all with variations in fibril orientations [18].

A second issue, apart from the magic-angle effect, that should be accounted for is the multi-exponential T2 behavior of articular cartilage. A study by Mlynarik et al. [51] suggested a bi(multi)exponential T2 behavior, with a short T2 component in the first 10 ms. These ultrashort T2 values are not resolved with most clinically used techniques and thus accounting for erroneously high values [46].

In acquiring T2 maps of articular cartilage, classically a multi-echo spin-echo sequence is used, followed by T2 map calculation with a non-linear (i.e., mono-exponential) fitting algorithm. As described for T1 mapping, color-encoded post-processing is used to render images de visu interpretable (Fig. 6). Several investigators have measured the spatial distribution of T2 relaxation times within cartilage. They all observe an overall decreasing trend going from the surface to depth. Despite differences in used methodology, there is a relatively good correspondence in obtained T2 values (Table 2) [35, 37, 42, 48, 52].

Aging appears to be associated with an asymptomatic increase in T2 relaxation times in the "transitional zone" [37]. This finding, together with the described angular T2 increase, should be considered in the differentiation between normal and pathological T2 increase when interpreting T2 maps. Three different patterns of pathological T2 were suggested by Mosher et al. [37]: (a) focal increased T2 confined to the radial zone; (b) heterogeneously elevated T2 extending to the articular surface; and (c) a focal cartilage tear with associated change in the spatial T2 distribution.

Magnetization transfer imaging

Cartilage, as a highly organized tissue, demonstrates the effects of MT [52]. It is based on the existence of two "pools" of hydrogen spins: those associated with colla-

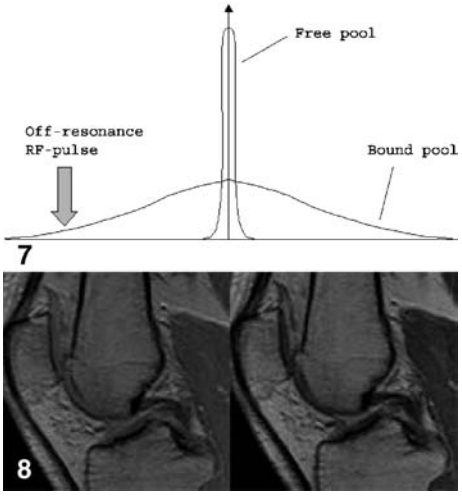

Fig. 7 Principles of MT imaging: in cartilage, two pools of water exist in constant exchange. The "bound" pool has an extremely short T2 relaxation time and broad line width. Saturation of the bound pool with an off-resonance radio-frequency pulse results in decreased signal from the "free" pool after exchange

Fig. 8 The 3D spoiled gradient-recalled-echo images (TR 45 ms/TE 4.4 ms/flip angle 12°) of articular cartilage without (*left*) and with (*right*) magnetization transfer. The decrease in cartilage and muscle signal is seen but is not present in the fat

gen fibers are considered the "bound" pool and those in water are the "free" pool. The MT imaging uses an off-resonance radio-frequency pulse to saturate the macromolecular bound hydrogen spins. They then exchange with free water spins, decreasing the overall signal intensity in regions where tight hydrogen-macromolecular coupling exists, i.e., in intact matrix collagen (Fig. 7). This decrease in signal, the MT rate, is tissue specific (e.g., high in muscle and cartilage, low in fat and fluid; Fig. 8).

The MT pulse can be added to every MR imaging sequence [53]. In practice, gradient-echo techniques are most often used. Two data sets are often required, one with MT saturation on and one with it off, followed by image subtraction. As opposed to the signal drop in normal cartilage, a region with disruption of the collagen framework is supposed to show increased signal due to a lower MT effect. Consequently, the subtracted image of this pathological region appears dark. Major disadvantages of this subtraction tool is patient motion between the two acquisitions leading to subtraction artifacts.

Despite the high specificity of the MT imaging technique for collagen matrix damage, Hohe et al. [54] stressed the important inter-individual as well as the intra-individual differences in MT rate. This may preclude its use in clinical applications.

Moreover, the two-proton pool model (i.e., free and bound pool) might be too simplified for cartilage MT imaging [55]. A four-site exchange system (comprising bulk water, collagen related water, collagen fibrillar water, and proteoglycan-related water) is proposed as an accurate model for cartilage relaxation and inter-spin group coupling. The actual clinical MT imaging only evaluates the collagen–bulk water subsystem, despite that the other coupling subsystems may be more relevant in early osteoarthritis. The authors state that new MT imaging techniques should be developed to focus on the other coupling subsystems to detect molecular abnormalities in the clinical setting of early osteoarthritis.

Magic-angle imaging

Magic-angle imaging, wherein the angular dependence of T2 is measured, provides a specific indication of collagen ultrastructure [18, 34, 44, 50, 56, 57]. This technique uses the magic-angle effect by placing the normal axis of the cartilage approximately 55° with respect to B_0. The difficulty in getting the exact angle, as patients cannot be turned in the magnet, precludes its use clinically, although it is likely to become a practical method for in vitro applications.

The third group of techniques are related to the interstitial water content of cartilage and comprise proton-density (PD) mapping and diffusion imaging.

Proton-density mapping

Mapping the spin density of articular cartilage is directly related to the interstitial water content. It is obtained as a by-product from either T1 or T2 measurements. The water content can be quantified by ensuring negligible T1/T2/diffusion and calibrating to a known water phantom. The use of phantoms is mandatory since proton-density (PD) measurements are always relative [58]. Additional factors need to be concerned, precluding the practical use of PD mapping: PD measurements should be corrected for focal solid matrix density; secondly, inherent relaxation processes affect the calculated PD, especially fast T2 decay [58]. Moreover, PD mapping reflects only the MRI detectable water and thus obscuring other water fractions which inevitably play a role in the disease process. Further research seems necessary to evaluate this highly sensitive but practical challenging technique.

Diffusion imaging

Self-diffusion of water provides a possible strategy for measuring water content because diffusivity is very sensitive to hydration [59]. The ability of water (and other

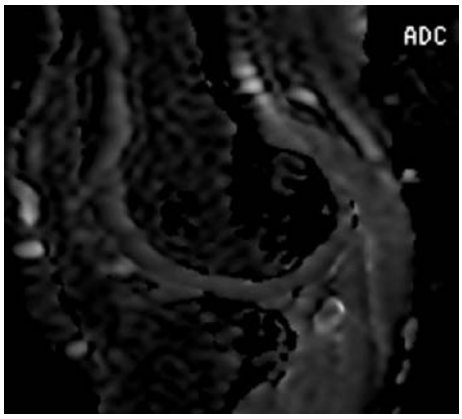

Fig. 9 Example of an apparent diffusion coefficient map of cartilage calculated from a diffusion-weighted technique based on single-shot spin-echo echo-planar imaging (TR 993 ms/TE 46 ms/ b=0, 370/no. of excitations=32). As is seen, this calculated image suffers from a low signal-to-noise ratio and motion incongruities

solutes) to move through cartilage is important because cartilage is an avascular tissue. The apparent diffusion coefficient (ADC) increases with proteoglycan and collagen depletion [60, 61] and has been related to degenerated human cartilage ex vivo [36]. To obtain a calculated ADC map, in which the signal intensity is proportional to the diffusivity, a series of images is acquired with different applied diffusion gradients (termed by the b-value). The diffusion gradients will induce a net phase change for moving spins depending on the distance they moved, resulting in signal loss.

The steric hindrance of the extracellular matrix (volume fraction, composition) is an important determinant for the diffusivity, explaining the ADC increase in diseased cartilage. The specific relationship, however, has yet to be determined [60]. An extended application of ADC mapping is diffusion tensor (i.e., fractional anisotropy) mapping, which gives an estimate of diffusion anisotropy. In normal cartilage, diffusion seems isotropic [60]. Cartilage matrix damage probably alters the diffusion anisotropic in analogy to the experiments performed by Quinn et al. [62].

In vivo diffusion measurements of cartilage are a huge challenge in the field of cartilage imaging, especially due to tissue anisotropy and limited resolution. Major drawback is the short T2 relaxation time of cartilage, necessitating a short echo time (TE) to maximize the cartilage signal. Applying diffusion-sensitizing gradients, however, increase the TE and render the sequence sensitive to motion; therefore, motion correction is often required before accurate reconstruction can be done [63]. Diffusion-weighted single-shot spin-echo echo-planar imaging is a frequently used technique for diffusion imaging (Fig. 9).

Conclusion

The described ultrastructural MRI techniques provide a probe to give information on cartilage which is inaccessible with any other non-invasive modality. Articular cartilage is a unique tissue from an MRI point of view: it consists out of a highly ordered collagen network, responsible for its T2 orientational dependence, and charged hydrophilic GAGs responsible for its T1 relaxation behavior in the presence of a charged MRI contrast agent.

For the evaluation of articular cartilage, specific methods should be used: three methods permit a very specific measure of the cartilage biochemical state: PD mapping directly measures water content, magic-angle imaging is a specific measure of collagen ultrastructure and charge-based methods (either dGEMRIC or sodium MRI) provide a specific measure of the GAG distribution.

For practical clinical applications, the whole picture seems less attractive: out of the specific techniques, only dGEMRIC can be used when keeping in mind abovementioned drawbacks and major disagreements in literature concerning resulting T1 values. For the evaluation of the collagen component, the less specific technique of T2 mapping is used, and although a correlation is found between MT rate and collagen damage, it still remains unclear whether this technique has sufficient sensitivity and specificity to be used in clinical cartilage imaging. The evaluation of the water component poses even more problems, as the clinical use of diffusion imaging seems precluded because of limited resolution and motion artifacts.

Concerning clinical imaging of articular cartilage the overall long acquisition schemes (i.e., patient motion), the 2-h interval needed for dGEMRIC and the need for image post-processing preclude a widespread use in daily clinical practice. Suggested solutions might be the use of higher field systems (3 T); however, susceptibility artifacts, inevitably present in each patient after surgical cartilage repair procedures, are enforced in higher field systems and thus possibly disabling correct image interpretation. Further work is necessary to deal with this issue. Another approach might be to limit the field of view to a specific cartilage area, enabling the shortage of acquisition time or the use of small surface coils to improve the signal-to-noise ratio.

Although these conclusions seem disenchanting for clinical cartilage imaging, further refinement of existing methods and development of new techniques may in the event lead to imaging protocols ready for daily use able to reveal both the morphology and biochemical content of cartilage lesions and cartilage repair tissue.

References

1. Cooper C (1995) Occupational activity and the risk of osteoarthritis. J Rheumatol 43:10–12
2. Disler DG, McCauley TR, Kelman CG, Fuchs MD, Ratner LM, Wirth CR, Hospodar PP (1996) Fat-suppressed three-dimensional spoiled gradient-echo MR imaging of hyaline cartilage defects in the knee: comparison with standard MR imaging and arthroscopy. AJR 167:127–132
3. Daenen BR, Ferrara MA, Marcelis S, Dondelinger RF (1998) Evaluation of patellar cartilage surface lesions: comparison of CT arthrography and fat-suppressed FLASH 3D MR imaging. Eur Radiol 8:981–985
4. Bredella MA, Tirman PF, Peterfy CG, Zarlingo M, Feller JF, Bost FW, Belzer JP, Wischer TK, Genant HK (1999) Accuracy of T2-weighted fast spin-echo MR imaging with fat saturation in detecting cartilage defects in the knee: comparison with arthroscopy in 130 patients. AJR 172:1073–1080
5. Suh JS, Lee SH, Jeong EK, Kim DJ (2001) Magnetic resonance imaging of articular cartilage. Eur Radiol 11:2015–2025
6. Imhof H, Nobauer-Huhmann IM, Krestan C, Gahleitner A, Sulzbacher I, Marlovits S, Trattnig S (2002) MRI of the cartilage. Eur Radiol 12:2781–2793
7. Sonin AH, Pensy RA, Mulligan ME, Hatem S (2002) Grading articular cartilage of the knee using fast spin-echo proton density-weighted MR imaging without fat suppression. AJR 179:1159–1166
8. Mohr A, Priebe M, Taouli B, Grimm J, Heller M, Brossmann J (2003) Selective water excitation for faster MR imaging of articular cartilage defects: initial clinical results. Eur Radiol 13:686–689
9. Gold GE, Bergman AG, Pauly JM, Lang P, Butts RK, Beaulieu CF, Hargreaves B, Frank L, Boutin RD, Macovski A, Resnick D (1998) Magnetic resonance imaging of knee cartilage repair. Top Magn Reson Imaging 9:377–392
10. Alparslan L, Minas T, Winalski CS (2001) Magnetic resonance imaging of autologous chondrocyte implantation. Semin Ultrasound CT MR 22:341–351
11. Recht M, White LM, Winalski CS, Miniaci A, Minas T, Parker RD (2003) MR imaging of cartilage repair procedures. Skeletal Radiol 32:185–200
12. Buckwalter JA, Mankin HJ (1997) Articular cartilage. I. Tissue design and chondrocyte matrix interactions. J Bone Joint Surg Am 79:600–611
13. Buckwalter JA, Mow VC (1992) Cartilage repair in osteoarthritis. In: Moskowitz RW, Howell DS, Goldberg VM, Mankin HJ (eds) Osteoarthritis. Saunders, Philadelphia, pp 71–107
14. Mankin HJ, Brandt KD (1992) Biochemistry and metabolism of articular cartilage in osteoarthritis. In: Moskowitz RW, Howell DS, Goldberg VM, Mankin HJ (eds) Osteoarthritis. Saunders, Philadelphia, pp 109–154
15. Benninghoff A (1925) Form und Bau der Gelenkknorpel in ihren Beziehungen zur Funktion. Anat Entwicklungsgesch 76:43
16. Jeffery AK, Blunn GW, Archer CW, Bently G (1991) Three-dimensional collagen architecture in bovine articular cartilage. J Bone Joint Surg Br 73:795–801
17. Clark JM (1991) Variation of collagen fiber alignment in a joint surface: a scanning electron microscope study of the tibial plateau in dog, rabbit, and man. J Orthop Res 9:246–257
18. Goodwin DW, Zhu H, Dunn JF (2000) In vitro MR imaging of hyaline cartilage: correlation with scanning electron microscopy. AJR 174:405–409
19. Bashir A, Gray ML, Burstein D (1996) Gd-DTPA2 as a measure of cartilage degradation. Magn Reson Med 36:665–673
20. Bashir A, Gray ML, Boutin RD, Burstein D (1997) Glycosaminoglycan in articular cartilage: in vivo assessment with delayed Gd-DTPA2-enhanced MR imaging. Radiology 205:551–558
21. Trattnig S, Mlynarik V, Breitenseher M, Huber M, Zembsch A, Rand T, Imhof H (1999) MRI visualization of proteoglycan depletion in articular cartilage via intravenous administration of Gd-DTPA. Magn Reson Imaging 17:577–583
22. Burstein D, Velyvis J, Scott KT, Stock KW, Kim YJ, Jaramillo D, Boutin RD, Gray ML (2001) Protocol issues for delayed Gd-DTPA2-enhanced MRI (dGEMRIC) for clinical evaluation of articular cartilage. Magn Reson Med 45:36–41
23. Tiderius CJ, Olsson LE, Verdier H de, Leander P, Ekberg O, Dahlberg L (2001) Gd-DTPA2-enhanced MRI of femoral knee cartilage: a dose-response study in healthy volunteers. Magn Reson Med 46:1067–1071
24. Gillis A, Bashir A, McKeon B, Scheller A, Gray ML, Burstein D (2001) Magnetic resonance imaging of relative glycosaminoglycan distribution in patients with autologous chondrocyte transplants. Invest Radiol 36:743–748
25. Nieminen MT, Rieppo J, Silvennoinen J, Toyras J, Hakumaki JM, Hyttinen MM, Helminen HJ, Jurvelin JS (2002) Spatial assessment of articular cartilage proteoglycans with Gd-DTPA-enhanced T1 imaging. Magn Reson Med 48:640–648
26. Stevens K, Berger F, Yoshioka H, Steines D, Genovese M, Lang P et al. (2001) Contrast-enhanced MRI measurements of GAG concentrations in articular cartilage of knees with early osteoarthritis. Proc 87th Scientific Assembly and Annual Meeting of the Radiological Society of North America, RSNA 2001. Radiology 221(P):288
27. Duewell SH, Ceckler TL, Ong K, Wen H, Jaffer FA, Chesnick SA, Balaban RS (1995) Musculoskeletal MR imaging at 4 T and at 1.5 T: comparison of relaxation times and image contrast. Radiology 196:551–555
28. Donahue KM, Burstein D, Manning WJ, Gray ML (1994) Studies of Gd-DTPA relaxivity and proton exchange rates in tissue. Magn Reson Med 32:66–76
29. Duvvuri U, Reddy R, Patel SD, Kaufman JH, Kneeland JB, Leigh JS (1997) T1-rho-relaxation in articular cartilage: effects of enzymatic degradation. Magn Reson Med 38:863–867
30. Duvvuri U, Kudchodkar S, Reddy R, Leigh JS (2002) T1-rho-relaxation can assess longitudinal proteoglycan loss from articular cartilage in vitro. Osteoarthritis Cartilage 10:838–844
31. Duvvuri U, Charagundla SR, Kudchodkar SB et al. (2001) Human knee: in vivo T1ρ-weighted MR imaging at 1.5 T—preliminary experience. Radiology 220:822–826
32. Reddy R, Insko EK, Noyszewski EA, Dandora R, Kneeland JB, Leigh JS (1998) Sodium MRI of human articular cartilage in vivo. Magn Reson Med 39:697–701
33. Borthakur A, Shapiro EM, Beers J, Kudchodkar S, Kneeland JB, Reddy R (2000) Sensitivity of MRI to proteoglycan depletion in cartilage: comparison of sodium MRI and proton MRI. Osteoarthritis Cartilage 8:288–293
34. Fragonas E, Mlynarik V, Jellus V, Micali F, Piras A, Toffanin R, Rizzo R, Vittur F (1998) Correlation between biochemical composition and magnetic resonance appearance of articular cartilage. Osteoarthritis Cartilage 6:24–32

35. Dardzinski BJ, Mosher TJ, Li S, Van Slyke MA, Smith MB (1997) Spatial variation of T2 in human articular cartilage. Radiology 205:546–550
36. Frank LR, Wong EC, Luh WM, Ahn JM, Resnick D (1999) Articular cartilage in the knee: mapping of the physiologic parameters at MR imaging with a local gradient coil—preliminary results. Radiology 210:241–246
37. Mosher TJ, Dardzinski BJ, Smith MB (2000) Human articular cartilage: influence of aging and early symptomatic degeneration on the spatial variation of T2—preliminary findings at 3 T. Radiology 214:259–266
38. Nieminen MT, Toyras J, Rieppo J, Hakumaki JM, Silvennoinen J, Helminen HJ, Jurvelin JS (2000) Quantitative MR microscopy of enzymatically degraded articular cartilage. Magn Reson Med 43:676–681
39. Nieminen MT, Rieppo J, Toyras J, Hakumaki JM, Silvennoinen J, Hyttinen MM, Helminen HJ, Jurvelin JS (2001) T2 relaxation reveals spatial collagen architecture in articular cartilage: a comparative quantitative MRI and polarized light microscopic study. Magn Reson Med 46:487–493
40. Xia Y, Moody JB, Alhadlaq H (2002) Orientational dependence of T2 relaxation in articular cartilage: a microscopic MRI (microMRI) study. Magn Reson Med 48:460–469
41. Dardzinski BJ, Laor T, Schmithorst VJ, Klosterman L, Graham TB (2002) Mapping T2 relaxation time in the pediatric knee: feasibility with a clinical 1.5-T MR imaging system. Radiology 225:233–239
42. Smith HE, Mosher TJ, Dardzinski BJ et al. (2001) Spatial variation in cartilage T2 of the knee. J Magn Reson Imaging 14:50–55
43. Peto S, Gillis P (1990) Fiber-to-field angle dependence of proton nuclear magnetic relaxation in collagen. Magn Reson Imaging 8:705–712
44. Xia Y, Farquhar T, Burton-Wurster N, Lust G (1997) Origin of cartilage laminae in MRI. J Magn Reson Imaging 7:887–894
45. Mosher TJ, Smith H, Dardzinski BJ, Schmithorst VJ, Smith MB (2001) MR imaging and T2 mapping of femoral cartilage: in vivo determination of the magic angle effect. AJR 177:665–669
46. Mlynarik V (2002) Magic angle effect in articular cartilage. AJR 178:1287–1288
47. Goodwin DW, Dunn JF (2002) MR imaging and T2 mapping of femoral cartilage. AJR 178:1569–1570
48. Lehner KB, Rechl HP, Gmeinwieser JK, Heuck AF, Lukas HP, Kohl HP (1989) Structure, function, and degeneration of bovine hyaline cartilage: assessment with MR imaging in vitro. Radiology 170:495–499
49. Modl JM, Sether LA, Haughton VM, Kneeland JB (1991) Articular cartilage: correlation of histologic zones with signal intensity at MR imaging. Radiology 181:853–855
50. Xia Y, Moody JB, Burton-Wurster N, Lust G (2001) Qualitative in situ correlation between microscopic MRI and polarized light microscopy studies of articular cartilage. Osteoarthritis Cartilage 9:393–406
51. Mlynarik V, Degrassi A, Toffanin R, Vittur F, Cova M, Pozzi-Mucelli RS (1996) Investigation of laminar appearance of articular cartilage by means of magnetic resonance microscopy. Magn Reson Imaging 14:435–442
52. Henkelman RM, Stanisz GJ, Kim JK, Bronskill MJ (1994) Anisotropy of NMR properties of tissues. Magn Reson Med 32:592–601
53. Wolff SD, Balaban RS (1994) Magnetization transfer imaging: practical aspects and clinical applications. Radiology 191:199–202
54. Hohe J, Faber S, Stammberger T, Reiser M, Englmeier KH, Eckstein F (2000) A technique for 3D in vivo quantification of proton density and magnetization transfer coefficients of knee joint cartilage. Osteoarthritis Cartilage 8:426–433
55. Lattanzio PJ, Marshall KW, Damyanovich AZ, Peemoeller H (2000) Macromolecule and water magnetization exchange modeling in articular cartilage. Magn Reson Med 44:840–851
56. Grunder W, Wagner M, Werner A (1998) MR-microscopic visualization of anisotropic internal cartilage structures using the magic angle technique. Magn Reson Med 39:376–382
57. Cova M, Toffanin R, Frezza F, Pozzi-Mucelli M, Mlynarik V, Pozzi-Mucelli RS, Vittur F, Dalla-Palma L (1998) Magnetic resonance imaging of articular cartilage: ex vivo study on normal cartilage correlated with magnetic resonance microscopy. Eur Radiol 8:1130–1136
58. Shapiro EM, Borthakur A, Kaufman JH, Leigh JS, Reddy R (2001) Water distribution patterns inside bovine articular cartilage as visualized by ^{1}H magnetic resonance imaging. Osteoarthritis Cartilage 9:533–538
59. Potter K, Butler JJ, Horton WE, Spencer RG (2000) Response of engineered cartilage tissue to biochemical agents as studied by proton magnetic resonance microscopy. Arthritis Rheum 43:1580–1590
60. Burstein D, Gray ML, Hartman AL, Gipe R, Foy BD (1993) Diffusion of small solutes in cartilage as measured by nuclear magnetic resonance (NMR) spectroscopy and imaging. J Orthop Res 11:465–478
61. Xia Y, Farquhar T, Burton-Wurster N, Vernier-Singer M, Lust G, Helinski L (1995) Self-diffusion monitors degraded cartilage. Arch Biochem Biophys 323:323–328
62. Quinn TM, Dierickx P, Grodzinsky AJ (2001) Glycosaminoglycan network geometry may contribute to anisotropic hydraulic permeability in cartilage under compression. J Biomech 34:1483–1490
63. Butts K, Pauly J, De Crespigny A, Mosely M (1997) Isotropic diffusion-weighted and spiral-navigated interleaved EPI for routine imaging of acute stroke. Magn Reson Med 38:741–749